

## PERFORMANCE ANALYSIS OF PUMP AS TURBINE AT DIFFERENT SHAPES AND SIZES NON-FLOW ZONES AND BALANCE HOLES

Mr. Satyajit Kashinath Jare<sup>1</sup>, Mr. Atharv Bhalchandra Kale<sup>2</sup>, Mr. Saurabh Sunil Nangare<sup>3</sup>,  
Mr. Mahesh Jaysing Babar<sup>4</sup>, Mr. Shubham Dattatray Pawar<sup>5</sup>,  
Mr. Sanket Sanjaykumar Patil<sup>6</sup>, Mr. R.R. Gaji<sup>7</sup>

<sup>1,2,3,4,5,6</sup>Student, Department Of Mechanical Engineering, Annasaheb Dange College Of Engineering And Technology, Ashta, India.

<sup>7</sup>Guide, Department Of Mechanical Engineering, Annasaheb Dange College Of Engineering And Technology, Ashta, India.

### ABSTRACT

Micro hydropower projects are the best alternatives for electricity generation. These power plants can be installed on small streams, rivers, channels, etc. without causing any effect on the environment. But the only problem is the high cost. The cost of a conventional turbine is very high. Hence the use of pumps instead of turbines is the best solution. This concept is generally known as a pump as turbine i.e., PAT. But the efficiency of PAT is low compared to conventional turbines. To improve the efficiency of PAT, a back cavity is filled with material like wood, which avoid the water to enter inside non-flow zones of PAT. Because of this, the disk-friction losses get reduced which increases efficiency.

But it cannot increase the efficiency by a significant amount so if we add the balance holes on the impeller it results in a further increase in efficiency and also it reduces the pressure gap between the front and back cavities.

### 1. INTRODUCTION

#### Background

Energy is indisputable the key factor for today's economic and social development within nations. The provision of reliable, secure and affordable energy services is central to addressing many of today's global development challenges. A micro hydro power plant is a type of hydroelectric power plant that generates electricity using the power of flowing water. As the name suggests, it is a smaller scale hydroelectric power plant that can generate up to 100 kilowatts of electricity. hydropower plants (MHP) are useful for the electrification of rural community, remote locations etc. Micro hydro power plants are typically used in areas where there is a consistent supply of water flow, such as mountainous regions, and can provide a reliable source of electricity for off-grid communities or remote areas. They are considered to be environmentally friendly and sustainable, as they produce electricity without emitting greenhouse gases. However, they require a significant initial investment and require careful planning to ensure the water supply is sustainable and the installation is safe and efficient. The conventional turbines are very expensive for MHP. The cost of electro-mechanical turbines in MHP can reach up to 25% of the integral plant (Barbarelli *et al.*, 2017). In some cases, it can reach up to 60 % to 70 % of the total plant cost (Binama *et al.*, 2017). So, conventional turbines are not suitable for the MHP.

For micro-hydropower plants, Pump as turbine (PAT) is often to be cost effective solution over the conventional turbines. The PAT is simple in construction, small in size, easy to maintain and easily available at desired head and discharges. The pump can be used in the reverse mode like turbine without mechanical failure. A pump as turbine (PAT) is a device that can be used to generate electricity from flowing water in small scale hydropower systems. In contrast to traditional hydro turbines which are designed to convert the potential energy of water into electricity, PATs are designed to convert the kinetic energy of water into electricity. PATs work by reversing the flow of water through the impeller (the rotating part of the pump) and using it to drive a generator. The impeller blades are designed to operate in the opposite direction to those of a pump, allowing them to capture the energy of the water as it flows through the system. PATs can be used in a variety of applications, including small-scale off-grid power systems, irrigation systems, and renewable energy projects in rural areas. They are relatively simple and easy to install, making them a cost-effective solution for generating electricity from low-head hydro resources.

The efficiency of a PAT depends on a number of factors, for example the specific design of the impeller, the head and flow rate of the water, and the speed of rotation. With proper design and optimization, PATs can achieve efficiencies of up to 80%, making them a viable option for small-scale hydropower generation. But, to increase the reliability and life of the PAT, different forces acting on the impeller needs to be investigated separately. Generally, the pump manufacturers provide the data of axial and radial thrust generated on the impeller in the pump mode. In addition to

this, many researchers have investigated the net axial and radial forces on impeller at different operating condition of a pump. but very few researchers have investigated the axial and radial thrust on the pump as turbine. In order to research on the forces acting on the PAT impeller, literatures available in the pump mode is helpful.

### 1.2 Internal flow physics of PAT control volume

To understand detailed flow physics of PAT, the flow control volume is classified into 3 different zones. Namely, i) Flow zone, the main zone of PAT control volume contributing to shaft work. ii) Non-flow zone, the region of PAT control volume present between impeller hub and rear inner surface of casing (Back cavity) and impeller front shroud to front inner surface of casing (front cavity) doesn't contributing to generate shaft work and iii) Transition zone, present at the interfaces of flow zone and non-flow zone where the fluid from flow zone with fluid of non-flow zone (Doshi et al., 2018). Fig 1.1 shows the different zones of PAT control volume.

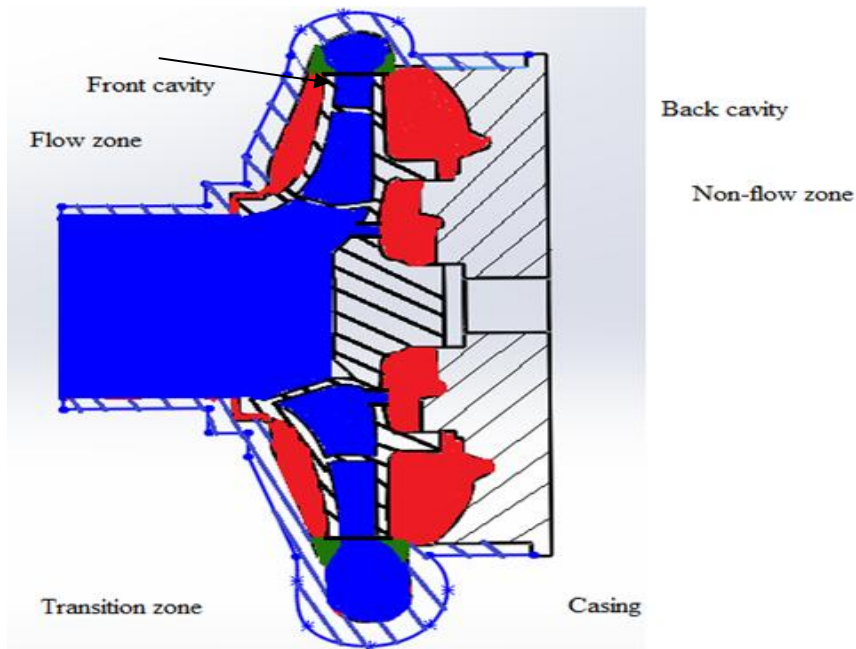


Fig. 1.1 Different zones of PAT control volume

#### Problem Statement

Singh (2005) focused on flow zone of PAT control volume and discussed various losses. Some researchers have done simple modifications of PAT without changing the basic design of pump that includes rounding of impeller blades with radius half of the thickness of blade (Singh, 2005, Suarda et al., 2006) and shrouds with radius half of the thickness of shroud (Derakhshan et al., 2009, Doshi et al., 2017), to reduce the suction wakes and to minimize the flow zone losses, providing external stationary ring to casing mouth for reduction of the local compression and shock waves due to contact between the fluid and rotating shroud, enlarging the suction eye for getting benefit of diffuser effect, removal of obstructions of flow like casing-eye ribs (Singh, 2005) etc. These all-simple modifications are related to flow zones of PAT control volume. But very few researchers are focused on non-flow zone of PAT.

In order to clearly understand the Impact of change in shape and size of non-flow zones on the performance of PAT, numerical investigation is important to be carried out which is not performed by the researchers. Moreover, the effect of BCF on the internal flow physics at various operating condition (part load, BEP, overload) of PAT is not Revealed so far. So it is important to optimize the size and shape of non-flow zones to improve the efficiency of PAT.

#### Objectives

By considering research background, objectives of this project work are set as below -

- To Determine overall efficiency of PAT.
- To determine axial thrust at different shapes and sizes of non-flow zones of PAT.
- To determine radial thrust at different shapes and sizes of non-flow zones of PAT.
- To analysis the effect of balance holes on the performance of PAT.

Solid works and Ansys fluent software have been Utilized as an effective tool to Estimate the performance and investigation for hydraulic losses in PAT.

#### Outcomes of project

Following are the expected outcomes

- The performance characteristics of PAT.
- To decrease disc-friction losses.
- To increase overall efficiency of Pump as Turbine (PAT).

## 2. LITERATURE REVIEW

CFD has been proven to be reliable tool to evaluate the characteristics of turbo machinery and to understand the complex flow structures in the fluid control volume. It saves design time and cost (Binama *et al.*, 2017). There are many researchers and scientists performed numerical simulation on PAT to understand the internal flow physics, predict the performance of PAT and optimization of PAT to improve the performance. In this section, detailed literature review based on numerical simulation is presented

**Baburaj et al., (2013)** analyze the performance of radial flow pump as turbine (specific speed 23.9 rpm) by performing numerical simulation in ANSYS-CFX. An unstructured meshing was done for impeller and volute. Draft tube, front cavity and back cavity were not considered for simulation. Boundary condition at inlet was total pressure and mass flow rate at outlet.

**Godbole, Vasant, Rajashree Patil, and S. S. Gavade.,** carried out the analysis of the axial thrust on centrifugal pump and concluded that important performance parameter for any is dependent on the hydraulic thrusts, Radial and Axial Thrusts.

**Kurokawa et al.,** published a research paper title as “A New Device to Control Axial Thrust of Radial Flow Turbomachinery”, in which they presented a simplified way to calculate axial force acting on impeller of pump and invented a device which control and also reduce the axial thrust of turbo machinery which having radial flow pattern.

**Derakhshan et.al. [1]** had performed the test on four industrial centrifugal pumps having specific speed in the range of 14-60 (m/s) to prove a prediction model for the best efficient point based on pump hydraulic characteristic. The efficiency in turbine mode was reported to be between 60 and 80%. The authors suggested that bigger pump impeller performs better in turbine mode.

**Guo et. al. [2]** had performed experimental investigation of a centrifugal pump with specific speed of 15.36 m/s operating it as turbine. From this experiment the best efficient point (BEP) was found at maximum head and mass flow rate than when it is operated in pump mode. The efficiency they obtain at 39%, head and mass flow of 30m and at the rate of 13.52 lps, respectively. The efficiency in pump mode was recorded 59%. From this they made concluded that hydraulic losses are higher when the pump is operated in turbine mode.

**Yang, Sun-Sheng et.al.[3]** worked on the effect of change in thickness of the blade of an impeller on Impact of PAT, they conducted the numerical research on PAT having different blade thickness at variable speed. By plotting (Q-H), (Q-P) and (Q-efficiency) they Noticed that as blade thickness decreases the efficiency increases.

**Doshi Ashish et.al.[4]** They carried out the work on the comparative effect of impeller blade and Impeller rounding. Impeller rounding is certainly beneficial and it had improved the operating efficiency from 0.5% to 2.5% at times.

**Liu and Tan, (2018)** investigated the effect of tip clearance between impeller blades and shroud on the performance of mixed flow pump in pump mode. Hexahedral structured grid is generated by ICEM-CFD. Refinement of grid was applied at the boundary of blade. A steady and transient simulation was performed by CFD code CFX 14.5 with SST-k<sub>o</sub> turbulence model. Boundary condition for this experiment at inlet was total pressure and mass flow rate at outlet.

**Barrio et al., (2010)** performed numerical investigation to check the flow pattern in the volute and impeller at different flow rates. Radial thrust on the impeller was estimated in pump and pump operated in reverse mode. Unsteady Reynolds Navier- Stokes equation was solved by CFD code Fluent. At designed flow rate, the flow was guided smoothly in the impeller passageways as shown in fig. 1 (b). Whereas the low-pressure region was observed at the blade passages for part load and overload conditions due to fluid recirculation. Interestingly, location of the flow reversal was observed near the pressure side of the blade region at part load condition as shown in fig. 1 (a) whereas this region was at the suction side of the blade tip for the overload region as shown in fig. 1 (c). For part load condition, radial thrust in PAT was less than pump mode. However, at overload condition radial thrust was found more than that of pump mode. It was further recommended to design the bearing and shaft carefully for the pump operated in reverse mode.

## 3. THEORETICAL MODEL

### 3.1 Theoretical models to analyze the performance of PAT

The formulas given by Doshi et al. (2018) to compare the externally measured variables (head, speed, torque and discharge) with internal hydraulics (losses and net rotational momentum) was shown below.

### 3.1.1 Torque at impeller or Euler head ( $H_E$ )

Torque at impeller or Euler head is the energy supplied by fluid to PAT at standard condition.

$$H_E = \frac{C_{u1}u_1 - C_{u2}u_2}{g}$$

$$\Delta C_\mu r = C_{\mu 1} r_1 - C_{\mu 2} r_2$$

For constant diameter and constant speed of PAT operation, peripheral speed of runner is constant.

$$H_E = \left( \frac{\Delta(C_u u)}{g} \right)_{impeller}$$

### 3.1.2 Net head (H)

Net head is the energy available between inlet and outlet section of PAT. Due to losses generated at flow zone, the torque at the impeller (head) or Euler head obtained less than net head.

$$H = \left( \frac{\Delta(C_u u)}{g} \right)_{impeller} + h_{L,fz} \quad \dots \dots \dots \quad 3.3$$

### 3.1.3 Shaft torque

At the end of the shaft of PAT the shaft torque measurement carried out, hence the losses in the non-flow zone and transition zone (neglecting the mechanical losses) must be taken under consideration. Therefore, the torque at the end of shaft can be evaluated by subtracting the non- flow zone and transition zone losses from torque at impeller.

Shaft torque = Torque at Impeller – loss of head in the non-flow zone – Loss of head in the transition zone

$$\left( \frac{\Delta(C_u u)}{g} \right)_{shaft} = \left( \frac{\Delta(C_u u)}{g} \right)_{impeller} - h_{L, \eta f z} - h_{L, \varepsilon z} \quad \dots \dots \dots \quad (3.4)$$

Where  $\left( \frac{\Delta(C_u u)}{g} \right)_{shaft} = \frac{T\omega}{\rho Q g}$

From equation (3.3) and (3.4), net head across the PAT control volume can be obtained as

$$H = \left( \frac{\Delta(C_u u)}{g} \right)_{\text{shaft}} + h_L$$

$$h_L = H - \left( \frac{\Delta(C_u u)}{g} \right)_{\text{shaft}} \dots \quad (3.6)$$

### 3.1.4 Axial thrust calculation

### *Axial thrust without balance hole*

To evaluate the axial thrust, the theoretical model proposed by Gulich (2014) is used. Axial force on impeller without balance hole is calculated by eq. (6).

$$F_{HY} = \frac{\pi}{4} (d_{sp}^2 - d_D^2) \left\{ \Delta P - \frac{\rho}{2} \bar{k}^2 u_2^2 \left( 1 - \frac{d_{sp}^2 + d_D^2}{2d_2^2} \right) \right\} \quad (6)$$

The axial force due to change in momentum is obtained from eq. (7).

$$F_I = \rho Q (C_{1m} - C_{2m} \cos \varepsilon_2) \quad (7)$$

Where  $\varepsilon_2$  is the angle between the outlet streamline and impeller axis.

The unbalanced axial force is presented by eq. (8)

$$F_w = \frac{1}{4} \pi d_D^2 (P_{amb} - P_1) \quad (8)$$

The net axial thrust on the impeller is then calculated from eq. (9)

$$F_A = F_{HY} - F_I + F_w \quad (9)$$

#### Axial thrust with no special design at the impeller back shroud

If there is no special design at the impeller shroud to reduce the axial thrust, the axial forces on the front shroud and rear shroud are calculated separately from eq. (10) and (11) respectively.

$$F_{FS} = \pi r_2^2 \left\{ \left( 1 - \left( \frac{d_{sp}}{d_2} \right)^2 \right) \Delta P - \frac{\rho}{4} u_2^2 c_{A,FS} \right\} \quad (10)$$

$$F_{RS} = \pi r_2^2 \left\{ \left( 1 - \left( \frac{d_D}{d_2} \right)^2 \right) \Delta P - \frac{\rho}{4} u_2^2 c_{A,RS} \right\} \quad (11)$$

Where  $C_A$  represents the coefficient of axial force reduction which is calculated from eq. (12) and (13)

$$c_{A,FS} = k_0^2 \left( 1 - \left( \frac{d_{sp}}{d_2} \right)^2 \right)^2 \quad (12)$$

$$c_{A,RS} = k_0^2 \left( 1 - \left( \frac{d_D}{d_2} \right)^2 \right)^2 \quad (13)$$

Where  $k_0$  is the rotation factor calculated as

$$k_0 = \frac{1}{1 + \left( \frac{r_w}{r_2} \right)^2 \sqrt{\left( \frac{r_w}{r_2} + 5 \frac{t_{ax}}{r_2} \right) \frac{c_{f,volute}}{c_{f,impeller}}}} \quad (14)$$

By using eq. (15) the net hydraulic force on the impeller in the axial direction is evaluated

$$F_{HY} = F_{RS} - F_{FS} \quad (15)$$

The force due to change in momentum, unbalanced axial thrust and net axial thrust on the impeller is calculated from eq. (7), (8), and (9) respectively.

#### Axial thrust with balance hole at the back shroud

In this stage, the hydraulic force on the impeller is first calculated without considering the balance holes as presented by eq. (6). For selected PAT,  $d_{s2}$  is larger than  $d_{sp}$  therefore the hydraulic force is evaluated from eq. (16),

$$F_{HY} = \frac{\pi}{4} (d_{sp}^2 - d_{s2}^2) \left\{ \Delta P - \frac{\rho}{2} \bar{k}^2 u_2^2 \left( 1 - \frac{d_{sp}^2 + d_{s2}^2}{2d_2^2} \right) \right\} \quad (16)$$

The net hydraulic force on the impeller is then calculated as,

$$F_{HY} = 0.1 - 0.2F_{HYeq.(6)} + F_{HYeq.(16)} \quad (17)$$

The net axial thrust is obtained as presented by eq. (9)

### 3.1.5 Radial thrust calculation

The radial thrust is calculated from the theoretical model proposed by Fernandez (2004).

$$F_R = P_2(b_2 + 2t)l \quad (18)$$

Where  $b_2$ ,  $t$  and  $l$  are the impeller outlet width, shroud thickness, and circumferential length, respectively in the pump mode.

## 4. NUMERICAL SIMULATION

### 4.1 Solid Modelling of PAT

Solid modelling is a technique used in computer-aided design (CAD) to create a three-dimensional (3D) virtual model of an object or a system. With the help of Computer Aided Design the actual prototype of PAT model can be generated with geometrical accuracy. Solid modelling allows the design, creation, visualization and animation of digital 3D models. In conclusion, solid modelling of a pump as a turbine requires careful consideration of key design features, material selection, and performance analysis. By taking these factors into account, an effective and efficient pump as a turbine can be designed.

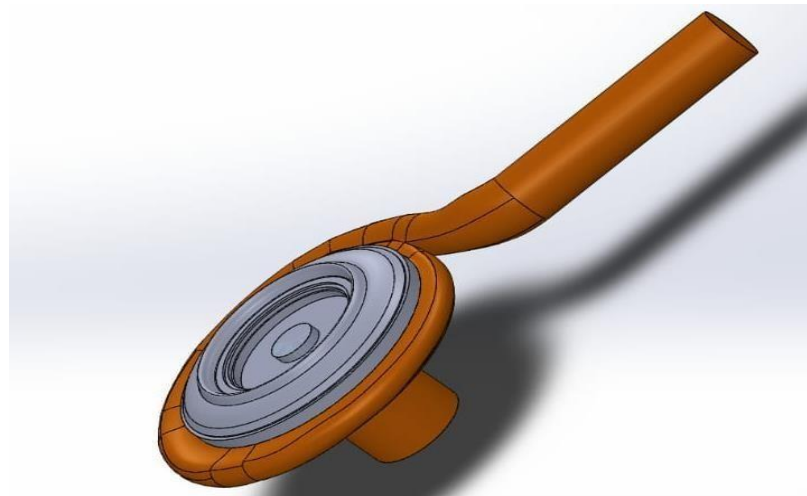


Figure 4.1 Solid model of PAT

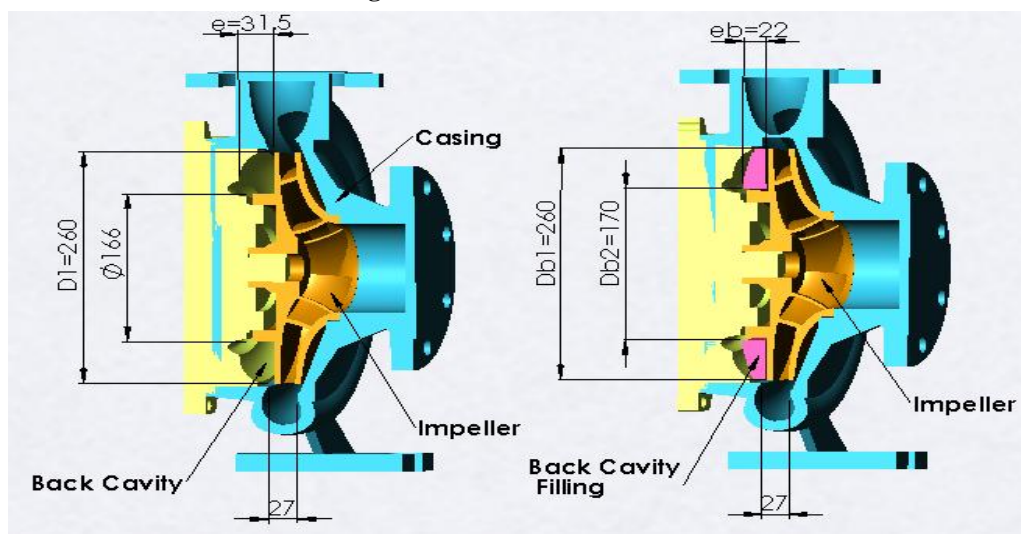
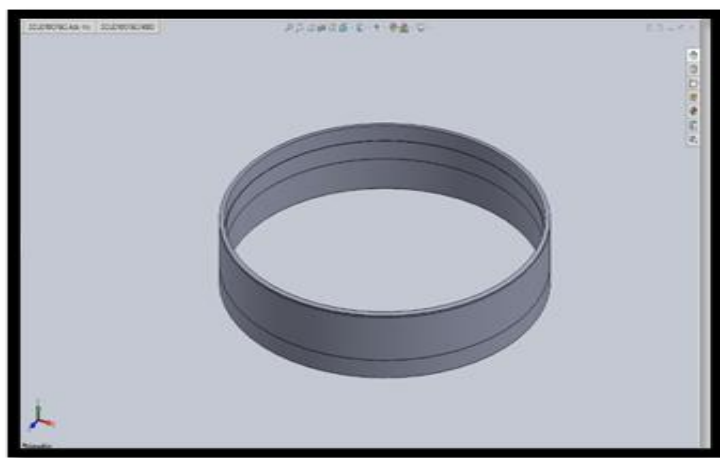


Fig. 4.2 Solid models of PAT without BCF and with BCF

(Doshi et al., 2018)

#### 4.2 Solid models of parts of Pump as Turbine



**Figure 4.3 Radial Clearance**

The radial clearance refers to the distance between the outer edge of the impeller blade and the inside of the volute casing. In a pump as a turbine (PAT) application, the radial clearance is an important consideration as it affects the performance and efficiency of the PAT.



**Figure 4.4 Back Plate**

A back plate of a pump can be used as a turbine by reversing the flow direction. When the pump is used to pump fluid, it plays the role of converting mechanical energy into fluid energy. However, when the flow direction of fluid is reversed, the back plate of the pump acts as a turbine by converting fluid energy into mechanical energy.

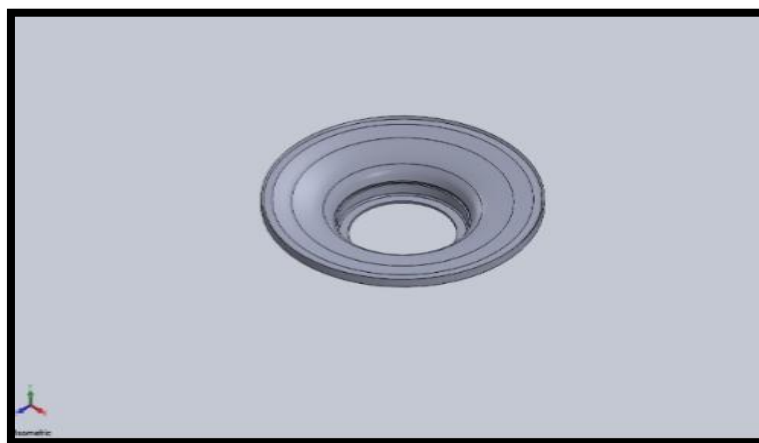


**Figure 4.5 Front Plate**

The front plate of a pump as a turbine (PAT) refers to the use of the front casing of a centrifugal pump as a turbine, which is also known as hydro-turbine. The concept of using pumps as turbines is based on the principle of Bernoulli's equation, which states that as the fluid flows through a narrowing channel, the velocity of the fluid increases, and the pressure decreases. This decrease in pressure can be utilized to generate electricity or mechanical power by coupling the turbine to a generator or a mechanical load, respectively.

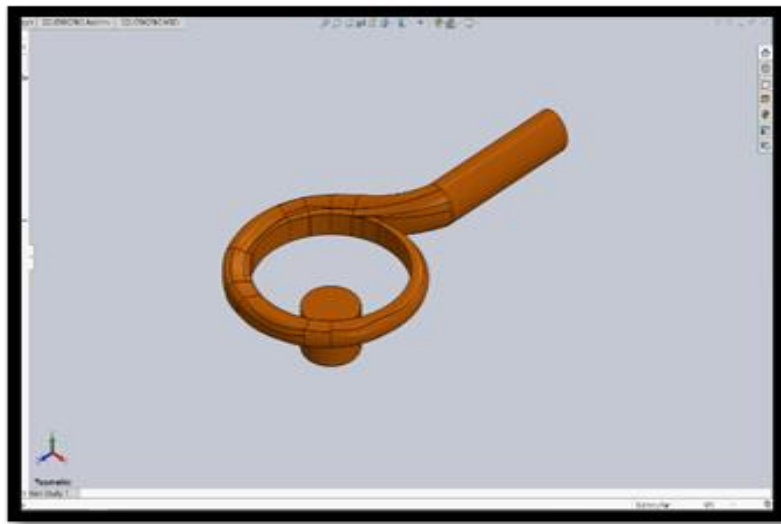


**Figure 4.6 Volute Casing**

The volute casing is designed to guide the flow out of the impeller, in order to convert the fluid flow's kinetic energy into static pressure it serves to collect the fluid discharged from the impeller and route it to the discharge nozzle (also see Pump casing).

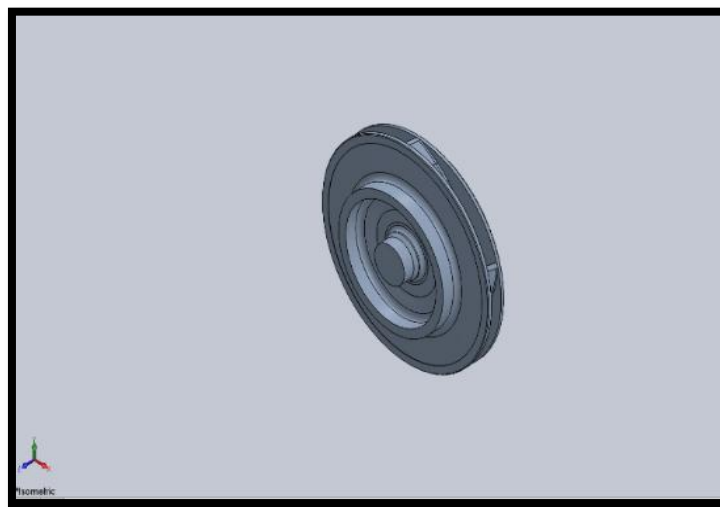


**Figure 4.7 Impeller**

An impeller is a rotating component of a centrifugal pump that accelerates fluid outward from the center of rotation, thus transferring energy from the motor that drives the pump to the fluid being pumped.[2] The velocity achieved by the impeller transfers into pressure when the outward movement of the fluid is confined by the pump casing. An impeller is usually a short cylinder with an open inlet (called an eye) to accept incoming fluid, vanes to push the fluid radially, and a splined, keyed, or threaded bore to accept a drive shaft.

#### 4.3 Computational Model of PAT

A computational model of a pump as a turbine (PAT) is typically used to simulate the performance of a pump being operated in reverse as a turbine. This model is important for designing micro-hydro power systems that use small-scale turbines, which often involve using pumps as turbines due to their cost-effectiveness and easy availability.

The computational model of a PAT involves simulating the fluid flow through the pump when it is operating in reverse as a turbine. This simulation can be performed using computational fluid dynamics (CFD) software, which involves solving the Navier-Stokes equations for fluid flow. To create a computational model of a PAT, the following

steps are typically taken: Geometric model creation: A 3D model of the pump and the surrounding fluid domain is created using a CAD software. Discretization: The fluid domain is discretized into small control volumes or cells using a meshing software. Boundary conditions: The boundary conditions are defined, such as flow rate, pressure, and rotational speed. Solver selection: A suitable CFD solver is selected based on the complexity of the system and the computational resources available.

Numerical solution: The Navier-Stokes equations for fluid flow are solved using the selected solver, and the results are computed. Post-processing: The simulation results are analyzed and presented in the form of diagrams and graphs. Validation: The computational model is validated against experimental data to ensure accuracy and reliability.

The computational model of a PAT can be used to optimize the design of turbines for maximum efficiency and performance. It can also be used to predict the performance of a proposed micro-hydro power system before it is built. In the numerical simulations, the actual geometry of the front and back cavity is considered, as shown in Fig. 2, which is not usually considered.

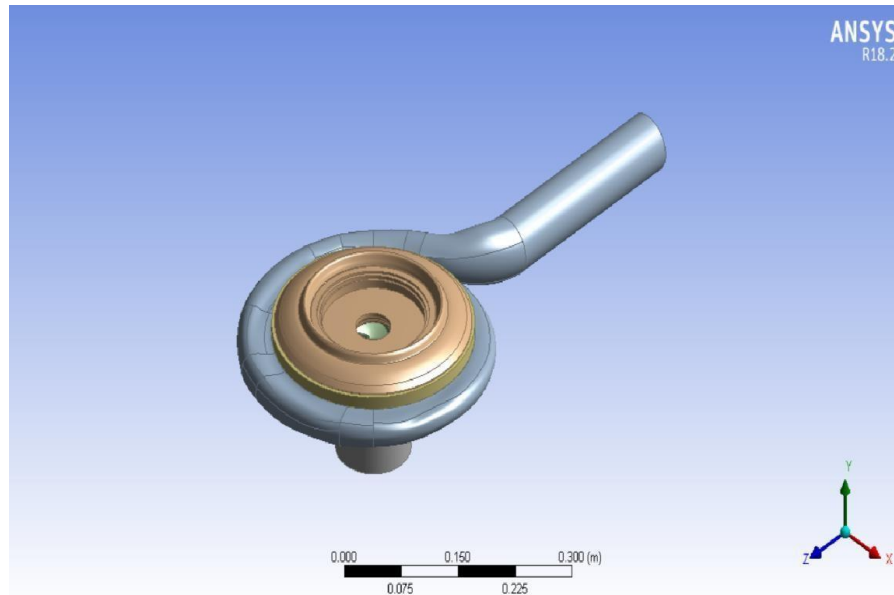


**Figure 4.8 Computational model of PAT**

#### 4.4 Mesh Generation

A tetrahedron mesh element is used to mesh the entire flow domain (Fernandez et al., 2009; Patil et al., 2018). The mesh elements are shown dense at the boundary region to find presence of boundary layer effect. The mesh at the blade profile is refined. The study of grid independence techniques is carried out to select the optimum number of mesh elements. The head and efficiency of PAT is obtained by varying the number of elements. The deviation in the head and efficiency is found to be 0.35% and 0.5% respectively at 3220215 numbers of elements. The  $y^+$  near the boundary wall is less than 35. Therefore, the same mesh size is applied for the simulations. Fig. 4.3 and Fig 4.4 shows tetrahedron mesh elements generated of the PAT and impeller of PAT.

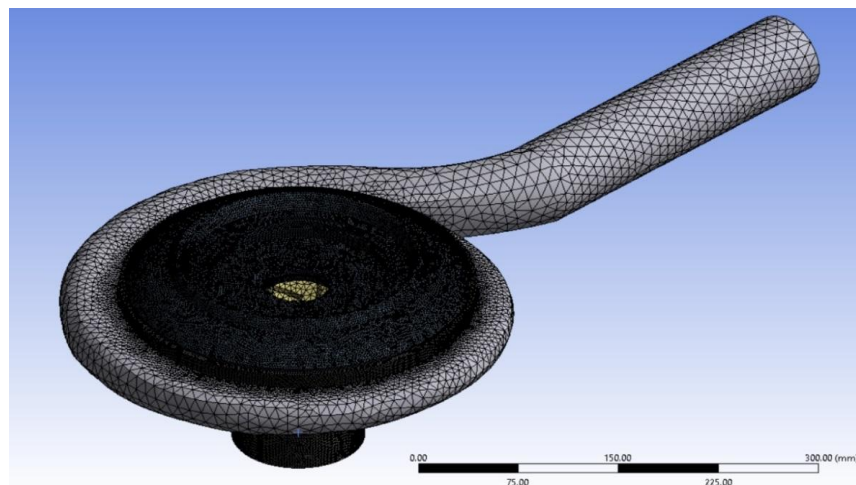


**Fig 4.9 Mesh generated on PAT**

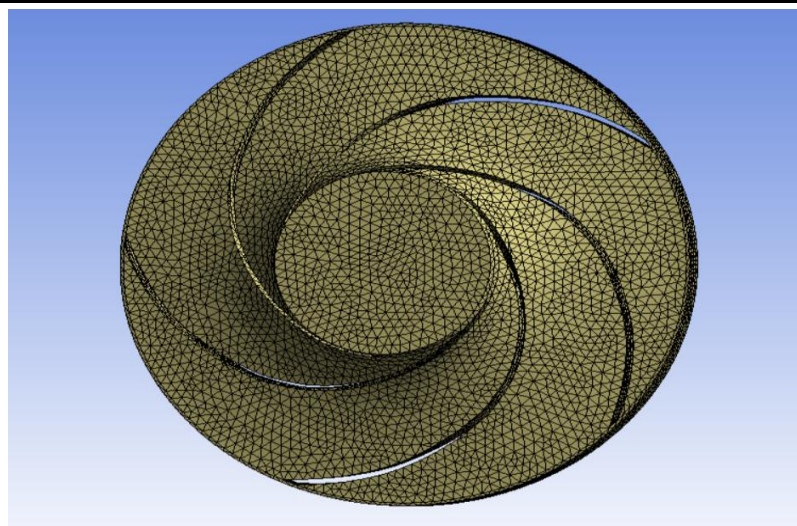


**Fig 4.10 Mesh generated on Impeller**

Mesh generation is the process to discretization the where the continuous domain is divided into the number of subdomains using different techniques of meshing. We have assigned the different sizes of mesh to the parts of PAT as per their complexity which is show below:

Type of Mesh                  Tetrahedron

Size:

- Volute Casing:                  10.0 mm
- Impeller:                  4.5 mm
- Pipe:                  1.8 mm
- Front Plate:                  1.8 mm
- Back Plate:                  1.8 mm
- Radial Clearance:                  1.8 mm

#### 4.4.1 Mesh Sensitivity Test

A mesh sensitivity test is a simulation process used to determine the effect of different mesh sizes on the accuracy and efficiency of a finite element analysis (FEA) model. It involves creating several versions of the same model using different mesh sizes and analysing the results to determine which mesh size produces the most accurate solution while minimizing computational time and resources.

The test typically involves running a simulation with a coarse mesh size, followed by an analysis with finer mesh sizes until reaching the optimal mesh size. The results of each analysis are compared to identify the mesh size that provides the most accurate results with the least computational effort. The optimal mesh size is a balance between accuracy and computational time and can vary depending on the specific application.

The mesh sensitivity test is a critical aspect of FEA modelling, as it ensures that simulation results are reliable and accurate. It helps engineers design more effective and efficient products by reducing the need for physical testing and improving the accuracy of virtual simulations. We have taken different mesh size for different parts of PAT model as per their complexity for the further calculation.

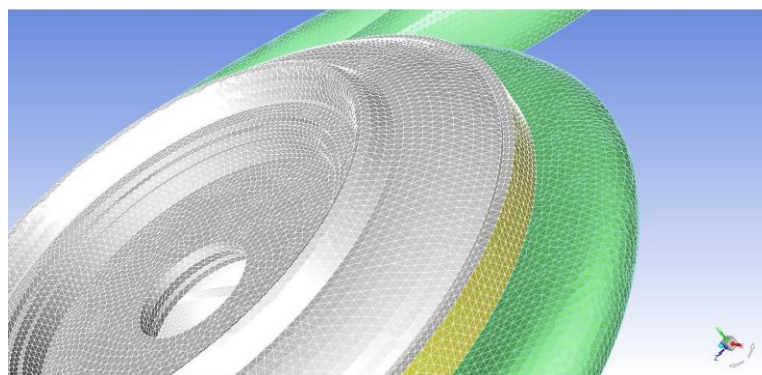


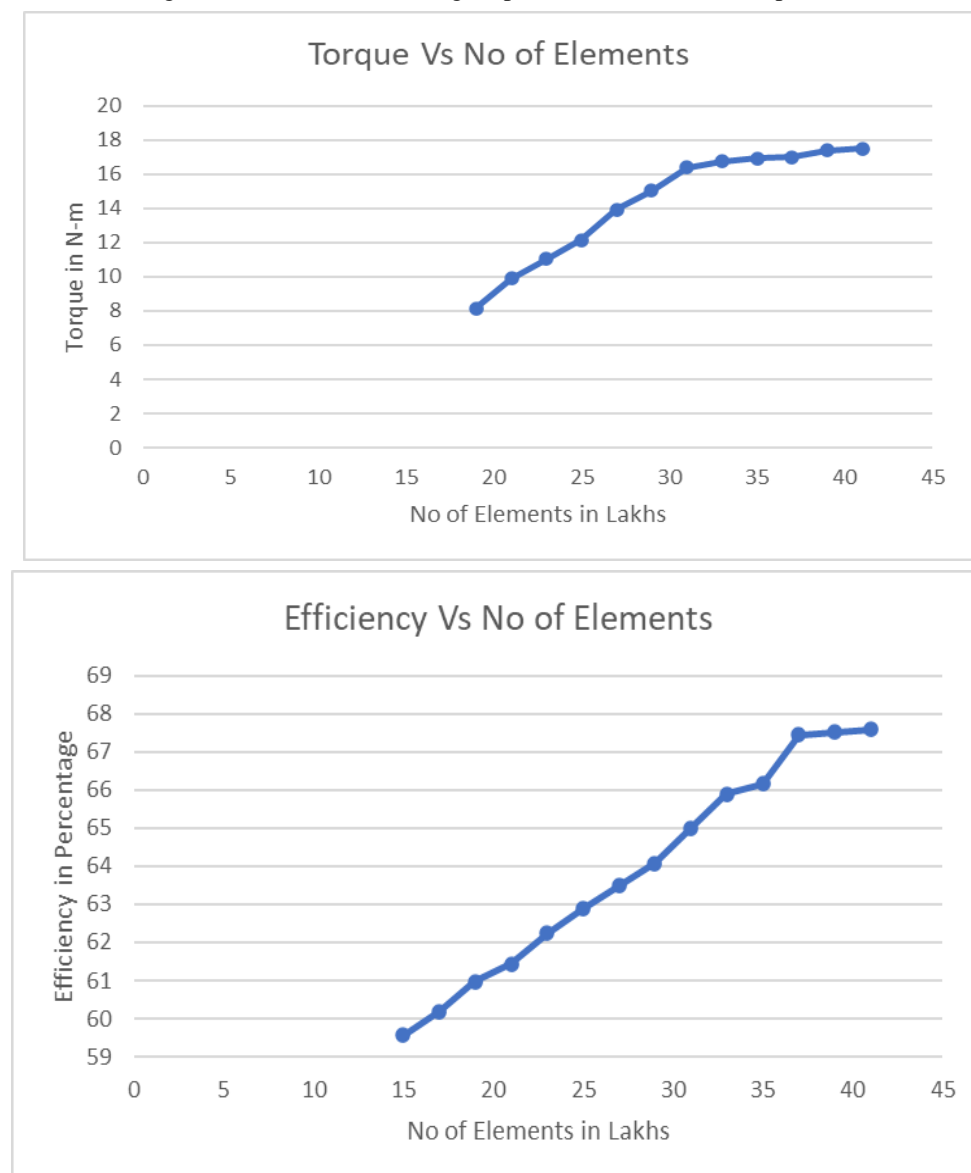
**Figure 4.11 Tetrahedron mesh elements**

### Mesh Sensitivity Test:

A mesh sensitivity test is a simulation process used to determine the effect of different mesh sizes on the accuracy and efficiency of a finite element analysis (FEA) model. It involves creating several versions of the same model using different mesh sizes and analysing the results to determine which mesh size produces the most accurate solution while minimizing computational time and resources.

The test typically involves running a simulation with a coarse mesh size, followed by an analysis with finer mesh sizes until reaching the optimal mesh size. The results of each analysis are compared to identify the mesh size that provides the most accurate results with the least computational effort. The optimal mesh size is a balance between accuracy and computational time and can vary depending on the specific application.

The mesh sensitivity test is a critical aspect of FEA modelling, as it ensures that simulation results are reliable and accurate. It helps engineers design more effective and efficient products by reducing the need for physical testing and improving the accuracy of virtual simulations. For this we have taken different mesh size for different parts of PAT model as per their complexity for the further calculation. It results in change in number of elements from 19 lakh to 50 lakh. So numerical simulation was carried out. After plotting the results on a graph, we get from 39 lakh mesh elements the curve was straight-line. From this test we get optimum mesh size for all parts.



#### 4.4.2 Turbulence Sensitivity Test

Depends on which turbulence model is chosen Numerical simulation results are form. Comparative study on several type of turbulence model is available by referring various turbulence models are investigated: (1)  $k-\omega$   
Subparts of above models are (1) SST

## SST k- $\omega$

We had taken the result by experimental & Numerical of turbulence model K-  $\omega$  SST, from that we have got the best efficiency point at 16.8 lps so we have selected K-  $\omega$  SST for our further calculation.

### 4.4 Governing Equations

In tensor form, the Reynolds-averaged governing equations for 3D, steady and incompressible turbulent flow with constant fluid properties are:

Continuity equation: 
$$\frac{\partial \overline{\rho u_j}}{\partial x_j} = 0$$

Momentum equation: 
$$\frac{\partial \overline{u_i}}{\partial t} + u_j \frac{\partial \overline{u_i}}{\partial x_j} = f_i - \frac{1}{\rho} \frac{\partial P}{\partial x_i} + \nu \frac{\partial^2 \overline{u_i}}{\partial x_j^2} + \frac{1}{\rho} \frac{\partial (-\rho \overline{u_i u_j})}{\partial x_j}$$

Where  $\overline{u_i}$ ,  $P$ ,  $\nu$  and  $\rho \overline{u_i u_j}$  are the time-averaged velocity, pressure, kinematic viscosity and stress tensor, respectively.

### 4.5 Numerical Simulation

Pump as turbine (PAT) is an emerging technology that utilizes pump units operated in reverse as hydraulic turbines to generate electric power. This technology has gained growing interest as an alternative energy source because it is cost-effective and environmentally friendly. Numerical simulation of the PAT is essential for its design and optimization.

The numerical simulation of a PAT mainly consists of the following steps:

Boundary conditions - The boundary conditions are applied to the model, which include the inlet flow rate and pressure, the outlet pressure, and the rotational speed of the impeller.

Fluid dynamics simulation - The simulation is then carried out using Computational Fluid Dynamics (CFD) software. The governing equations of fluid flow are solved, including the Navier-Stokes equations, continuity equations, and energy equations. The turbulent flow and the interactions between the rotating impeller and the stationary volute are also simulated.

Performance prediction - Performance metrics such as the head, efficiency, and power output of the PAT are predicted using the simulation results.

Optimization - The simulation results are analysed to identify design improvements that could increase the performance of the PAT. The optimization process may include changes in the impeller geometry, the volute shape, or the operational conditions of the PAT.

In summary, the numerical simulation of a PAT is a complex process that requires expertise in CFD and hydraulic engineering. The simulation results can be used to optimize the design and improve the performance of the PAT, which can lead to a more cost-effective and sustainable energy source. The Reynolds-averaged 3D Navier-Stokes equation is solved by

CFD code ANSYS-Fluent. The researchers commonly used two different turbulence models k- $\omega$  SST (Lin et al., 2021a, b) and k- $\epsilon$  (Yang et al., 2012a, b; Derakshan and Nourbakhsh 2008; Fernandez et al., 2009). The turbulence sensitivity test was conducted to select the appropriate turbulence model for the analysis. The efficiency of PAT is obtained at

k- $\omega$  SST, k-epsilon Realizable, k-epsilon standard, and k-epsilon RNG turbulence models and compared with the experimental results available for literatures (Doshi et al., 2018) as shown in Fig. 4. The efficiency calculated using the k- $\omega$  SST turbulence model matches with the experimental results. While, k-epsilon Realizable, k-epsilon standard, and k-epsilon RNG turbulence models are overestimated a efficiency. Therefore, the k- $\omega$  SST turbulence model is used for the numerical simulation.

The water is selected as a working fluid. At inlet of PAT pressure is given as boundary condition and at outlet mass flow rate is given. Surface roughness of the volute and impeller is 8.37 and 6.37 micron, respectively

The angular speed of the impeller taken as 1000 rpm. The same rotational speed is set to the impeller outer shroud surfaces (inner surface of back cavity and front cavity). The steady-state numerical simulations are performed. We had taken 300 iterations for each model of PAT.

### 4.6 Validation of the numerical results

The experimental results of low specific speed 19.9 rpm PAT are available (Doshi et al., 2018). Fig. 6 shows the comparison of numerical result of torque, head, and efficiency with the experimental results. Contained numerical

result are just slightly varied from the experimental results. All of the numerical results are in line with the experimental results. Numerical torque, head, and efficiency are consistently more than the experimental results. It may be due to the mechanical losses of seals and bearings are not considered in the simulation. The comparison of numerical and experiment results was carried out and CFD error is calculated.

## 5. RESULTS

### 5.1 Determination of Efficiency:

Table 5.1 Efficiency of PAT

PAT Model	P1 (Pa)	P2 (Pa)	Q (Kg/S)	T (N-m)	V1 (m/s)	V2 (m/s)	Head (m)	EFFICIENCY (%)
With BCF	143222.2	-14033.3	16.8	17.39076	4.831982	2.927601	16.78	67.5
Without BCF	143422.2	-6223.69	16.8	17.00927	4.837746	2.97414	16.00	65.8
With BCF & Balance Holes	143422.2	-562.854	16.8	17.50554	4.836381	2.711338	15.49	71.7
Without BCF & Balance Holes	143422.2	14152.85	16.8	15.55664	4.805823	2.79238	13.96	70.8

By using Ansys Fluent software and with the help of Computational Fluid Dynamics the simulation is carried out to find the overall efficiency. The results obtained are mentioned in the above table. Some performance parameters are obtained from Ansys Fluent like torque, pressure and velocity by following the procedure of general post processing. With the help of Bernoulli's equation head is calculated and after that efficiency value is evaluated. All results are mentioned in the above table.

Table 5.2 List of Axial thrust

PAT MODEL	F <sub>HY</sub> (N)	F <sub>I</sub> (N)	F <sub>w</sub> (N)	Axial thrust (N)	Radial Thrust (N)	η (%)
With BCF	1110.62	0.744	74.56	1110.6	135372.3	67.5
Without BCF	1058.15	0.781	71.15	1058.1	133824.4	65.8
Without BCF & Balance Holes	1148.96	0.868	77.89	1148.9	118139.1	70.8
With BCF & Balance Holes	1123.68	0.819	76.86	1123.6	152253.8	71.7

Axial thrust generates in the centrifugal pumps due to asymmetry. The gap between the impeller back shroud and casing inner cover, the impeller front shroud, and volute casing are filled with fluid(water) at high pressure. The pressure generated acts on the impellers face because the back shroud has a big surface area than of front cover, a net thrust is developed that acts in direction opposite to the flow of the fluid. Since, the net axial thrust is the common difference in the forces acts between the front and back shrouds. The axial thrust acting on the impeller of the PAT should check. Because change in size of non-flow zones could affect the forces acting on the impeller. Which result in change in axial thrust. Because of unbalanced axial thrust the vibration are generated inside the turbomachinery and affects the life, reliability and performance of turbomachinery. Hence to avoid this the evaluation and validation of axial thrust was carried out.

### 5.2 Validation of numerical results with experimental results

In case of numerical simulation approach, it is important to determine whether the results we obtained by performing the simulations with the help of computational fluid dynamic and ANSYS Fluent software are correct or not. For that the comparative test should be carried out between numerical results and experimental results. The validation of numerical results with experimental carried out and the error in the parameters like torque, head and efficiency is comes out up to 5 % which is nominal. Comparison of experimental results are carried out with the help of theoretical results from various research papers.

Table 5.3 Comparative Analysis of Experimental and Numerical Value

5.3 Pressure and Velocity Contours:

Parameters	With BCF		CFD Error %	Without BCF		CFD Error %
	Experimental	Numerical		Experimental	Numerical	
<b>Head</b>	16.78	17.02	1.43	16.00	16.72	4.5
<b>Torque</b>	17.39076	18.37	5.63	17.00927	17.12	0.65
<b>Efficiency</b>	67.5	68.15	3.57	65.8	64.55	4.37

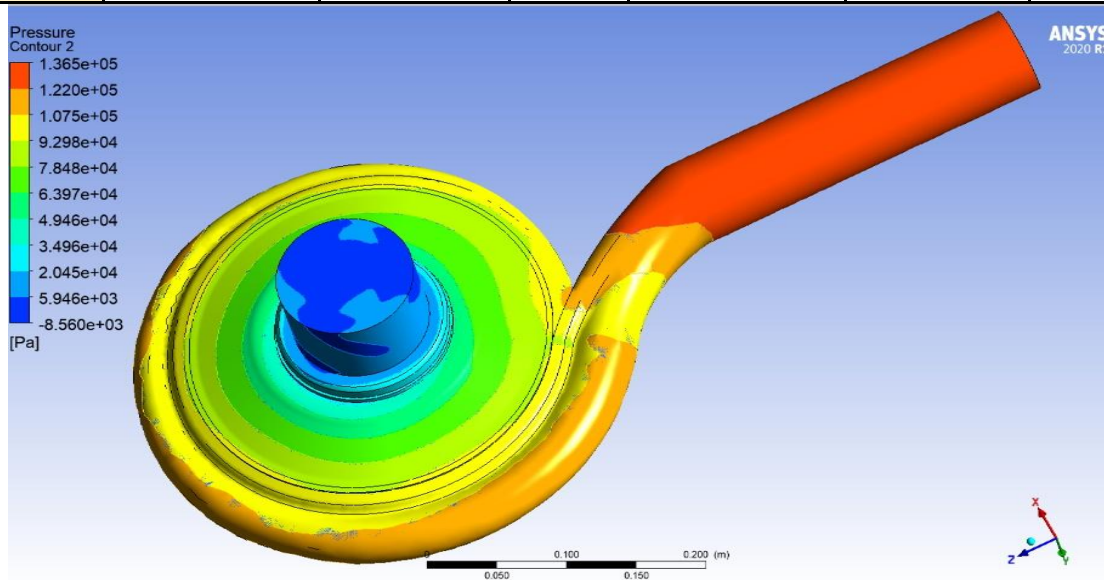
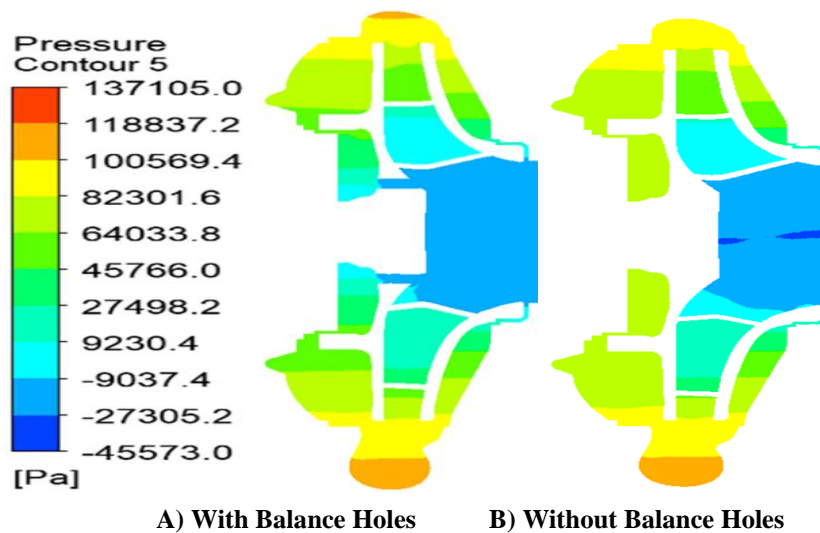
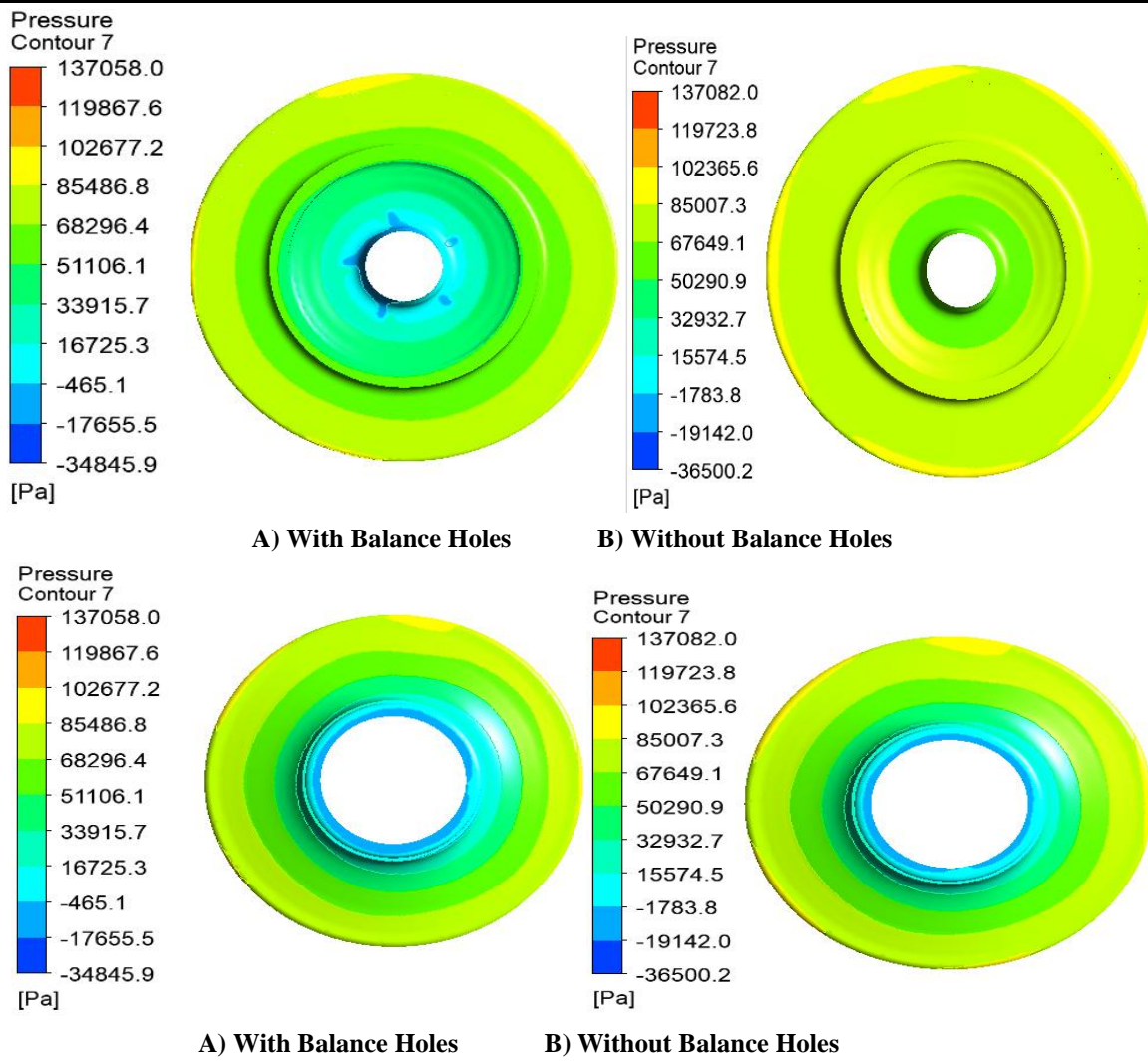


Figure 5.1 Pressure Contour

Above figure shows the pressure contour of PAT model in that the maximum pressure is to be obtained is  $1.365e+05$  Pa contact which is at inlet volute surface region. And the minimum pressure obtained is  $-8.560e+04$  which is at outlet pipe region. As the contact area increases the pressure get reduced. The flow pattern of fluid inside the pump is streamline. It follows the Bernoulli's Principle which state that the pressure energy, kinetic energy and hydrostatic energy of incompressible fluid remains always constant.



A) With Balance Holes      B) Without Balance Holes



**Figure 5.2 Pressure Contour of Mediatorial Plane**

In above fig the pressure contours of Mediatorial plane are shows, in which the maximum pressure is obtained at volute region from where the water is to be entered and the minimum pressure is to be obtained at the region of outlet of PAT model from pipe section. It can be seen from above pressure contours, the pressure gap between front and back cavity is minimized with the help of addition of balance holes. The addition of balance holes also leads to balance the axial thrust. By chance the water gets into the non-flow zones where back cavity filled with the material then balance holes present on impeller takes that water from non-flow zones to the flow zones of PAT. Which in results increase the life of Back cavity filling.

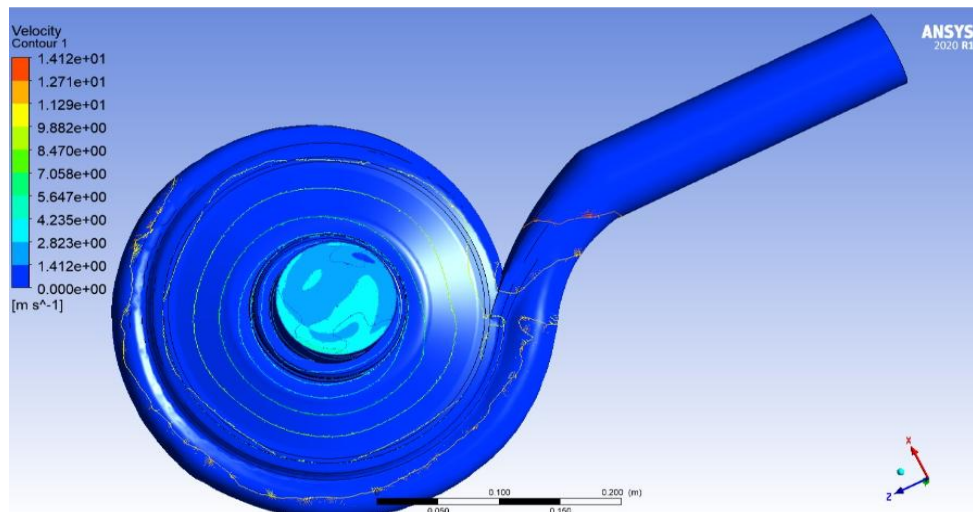


**Figure 5.3 Velocity Contours**

Above figure is of velocity contour shows the minimum and maximum value of velocity at different region, the maximum velocity is obtained at inlet region and minimum is at outlet region which is shown in this above figure. With the help of this values, we can get the efficiency at the last calculation.

## 6. CONCLUSIONS

In recent years, there has been an increasing interest in using pumps as turbines for energy generation. The ability to use a pump as a turbine provides an alternative to traditional hydropower generation using traditional turbines, which can be costly and require significant infrastructure. Pumps as turbines are now a viable option, especially in small hydropower generation projects where their suitability is evident. The higher efficiency of these systems, coupled with their ability to operate with a wide range of flows and heads make them more reliable than conventional turbines, thereby providing an attractive alternative for low-head hydropower generation. Further research will continue to improve the design and manufacturing of these systems, making them a more viable option for electricity generation from small water resources. Overall, the use of pumps as turbines is an excellent innovation in the development of sustainable energy systems.

To improve the efficiency of PAT, a back cavity is filled with material like wood, which avoid the water to enter inside non-flow zones of PAT. Because of this, the disk-friction losses get reduced which increases efficiency.

But it cannot increase the efficiency by a significant amount so if we add the balance holes on the impeller it results in a further increase in efficiency and also it reduces the pressure gap between the front and back cavities.

It is observed that back cavity filling improves the efficiency of PAT. All numerical results follow the trend of experimental results. As back cavity filling is carried out, the efficiency of PAT is increased by 1.7 %. If balance holes are created on the impeller, it increases the efficiency by 5% as compared to PAT having an impeller without balance holes. If balance holes are added to the impeller and also the back cavity is filled with some material it results in an increase in the efficiency of the Pump as a Turbine in a significant amount.

## 7. REFERENCES

- [1] Derakhshan, S. and Nourbakhsh, A. (2008) 'Theoretical, numerical and experimental investigation of centrifugal pumps in reverse operation', *Experimental Thermal and Fluid Science*, 32(8), pp. 1620–1627. doi: 10.1016/j.expthermflusci.2008.05.004.
- [2] Guo, S., Okamoto, H., & Maruta, Y. (2006). Measurement on the fluid forces induced by rotor-stator interaction in a centrifugal pump. *JSME International Journal Series B Fluids and Thermal Engineering*, 49(2), 434-442.
- [3] Yang, S., Kong, F., Fu, J. and Ling, X. (2012) 'Numerical Research on Effects of Splitter Blades to the Influence of Pump as Turbine', *International Journal of Rotating Machinery*, 2012. doi: 10.1155/2012/123093.
- [4] Doshi, A., Channiwala, S., & Singh, P. (2018). Influence of Nonflow Zone (Back Cavity) Geometry on the Performance of Pumps as Turbines. *Journal of Fluids Engineering*, 140(12).
- [5] Godbole, V., Patil, R., & Gavade, S. S. (2012, July). Axial thrust in centrifugal pumps—experimental analysis. In 15th International Conference on Experimental Mechanics, Porto/Portugal (pp. 22-27).
- [6] Ji, X. Y., Li, X. B., Su, W. T., Lai, X., & Zhao, T. X. (2016). On the hydraulic axial thrust of Francis hydro-turbine. *Journal of Mechanical Science and Technology*, 30(5), 2029-2035.
- [7] GÜLICH, J. F. (2014). Pump types and performance data. In *Centrifugal pumps* (pp. 43-78). Springer, Berlin, Heidelberg.
- [8] Couzinet, A., Gros, L., & Pierrat, D. (2013). Characteristics of centrifugal pumps working in direct or reverse mode: focus on the unsteady radial thrust. *International Journal of Rotating Machinery*, 2013.
- [9] Park, S. H., & Morrison, G. L. (2009, January). Analysis of the flow between the impeller and pump casing back face for a centrifugal pump. In *Fluids Engineering Division Summer Meeting* (Vol. 43727, pp. 221-235).
- [10] Rawal, S. and Kshirsagar, J. T. (2007) 'Numerical simulation on a pump operating in turbine mode', in proceedings of the twenty-third international pump user's symposium• 2007, pp. 21–28